Title

EXPLOSION-EVAPORATION MODEL FOR FRAGMENT PRODUCTION IN MEDIUM-ENERGY NUCLEAR COLLISIONS

Authors

Fai, G.
Randrup, J.

Publication Date

1981-10-01

LBL-13357
Preprint

Lawrence Berkeley Laboratory
UNIVERSITY OF CALIFORNIA

Submitted to Nuclear Physics A

EXPLOSION-EVAPORATION MODEL FOR FRAGMENT PRODUCTION IN MEDIUM-ENERGY NUCLEAR COLLISIONS

George Fái and Jørgen Randrup

October 1981

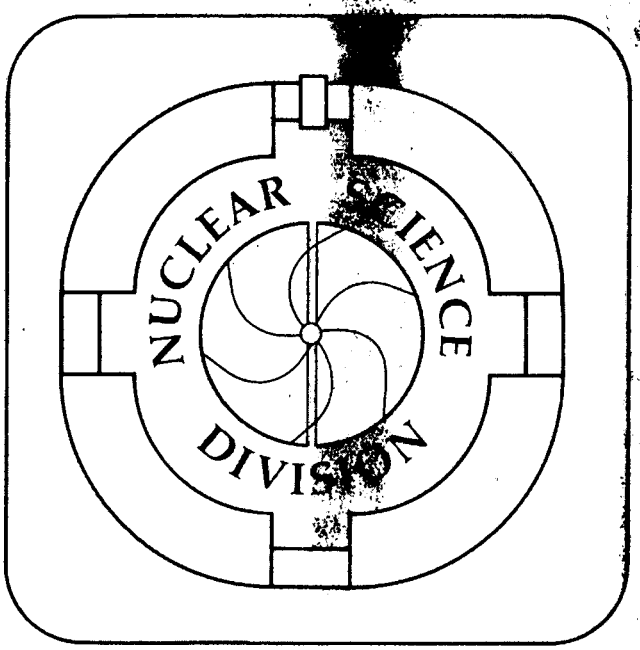

Prepared for the U.S. Department of Energy under Contract W-7405-ENG-48

DISCLAIMER

LBL-13357

Explosion-Evaporation Model for Fragment Production in Medium-Energy Nuclear Collisions*

George Fái† and Jørgen Randrup

Nuclear Science Division
Lawrence Berkeley Laboratory
University of California
Berkeley, CA 94720

October 1981

*This work was supported by the Director, Office of Energy Research, Division of Nuclear Physics of the Office of High Energy and Nuclear Physics of the U.S Department of Energy under Contract W-7405-ENG 48.

†On leave from the Roland Eötvös University, Budapest, Hungary

Abstract:

Statistical considerations are applied to the multifragment disassembly of a piece of hot nuclear matter created in medium-energy nuclear collisions. A two-stage model, consisting of a quick explosion and a slower evaporation, is presented. Results are compared to those of previous simpler calculations and to recent experimental data. The agreement is encouraging for a realistic range of the main parameters of the model: the available energy per nucleon, the isospin asymmetry, and the extension of the primary explosion in space and time.

1. Introduction

Several heavy-ion accelerators throughout the world are presently (or will soon be) able to deliver beams of heavy nuclei with kinetic energies in the range from tens to hundreds of MeV per nucleon. This development has stimulated increased experimental and theoretical activity in the field of medium-energy nuclear collisions. Ref. [1] recently pointed out the possibility of creating a transient nuclear system with an excitation comparable to its total binding energy. Such a hot nuclear system may decay into a large number of different multifragment channels. In the present paper we address this disassembly process.

The disassembly process is expected to be very complicated, and a detailed dynamical description is beyond our present capability. However, by virtue of the complexity of the process, statistical considerations may be useful, in particular when the interest is focused on single-particle inclusive quantities. A statistical model yields the least biased estimates about the disassembly process and provides a meaningful reference against which more specific dynamical models can be discussed.

Statistical ideas were first applied to hadronic reactions by Fermi [2], who considered pion production in high-energy proton-proton collisions. For relativistic nuclear collisions Mekjian [3] and others [4,5] have developed models for composite fragment production assuming thermal and chemical equilibrium within a certain volume. Similar ideas were applied at medium energies by Koonin and Randrup [1].

In this latter work the accessible phase space for the disassembly process included only particle-stable nuclear states. However, the collision process also produces metastable nuclear fragments with half-lives long on the time scale characterizing the disassembly process. Therefore, it appears

desirable to extend the model to include unstable fragments in the statistical disassembly process. The subsequent decay of these fragments needs then to be also considered. Towards this end, we propose a two-stage idealization of the disassembly process. In the primary stage the system quickly "explodes" into single nucleons and composite nucleides (at higher energy the creation of pions may also be important), according to the available phase space. In the secondary stage the unstable nucleides produced in the explosion "evaporate" light ejectiles, such as nucleons and alpha-particles, on a somewhat longer time scale. [Their later further deexcitation by way of electromagnetic radiation need not be considered since it does not change the relative fragment yields and has a negligible effect on the fragment spectra.] This model is described in Section 2. Section 3 discusses some instructive results and establishes contact with experiment. In Section 4 we make some concluding remarks. The Appendix addresses the relation between the volume parameter χ of the present model and the conventional "break-up" baryon density ρ.

2. Description of the model

The disassembly of a system of hot nuclear matter is idealized as a two-stage process. The primary, fast stage is referred to as the explosion, while the secondary, slower stage is denoted the evaporation. The treatment of the two stages is described below.

2.1 Explosion

Following ref. [1], we assume that the explosion populates phase space statistically. The evaluation of the exact microcanonical phase space is a formidable task. Substantial simplification can be achieved by invoking the grand canonical ensemble, as is justified for sufficiently large systems. The ensemble averages are then given in terms of the partition function

$$Z = \sum_f e^{-\beta(E_f - \mu A_f - \nu T_f)} \quad . \tag{1}$$

The sum extends over all possible final states f. The Lagrange multipliers β, μ, and ν are adjusted to ensure that the ensemble averages of the total energy E_f, the total baryon number A_f, and the total isospin component T_f be equal to the prescribed values E_o, A_o, and T_o.

It is advantageous to introduce the intensive quantity $\omega = (\ln Z)/A_o$. Neglecting the interactions between fragments, ω can be expressed in terms of contributions from different fragment species (characterized by AT): $\omega = \Sigma\omega_{AT}$. Each term is of the form

$$\omega_{AT} = \chi \frac{4\pi}{3} r_o^3 \left(2\pi \frac{mA}{\beta h^2}\right)^{3/2} \zeta_{AT} e^{-\beta(V_{AT} - \mu A - \nu T)} \tag{2}$$

The different factors in ω_{AT} arise from summation over different dimensions of phase space. The volume factor $\chi\frac{4\pi}{3}r_o^3$ is a result of the integration over fragment position and expresses the effectively available volume of the system at disassembly. The dimensionless parameter χ is the ratio of the available volume and the reference volume $\frac{4\pi}{3}r_o^3 A_o$. The relation of χ to the baryon density at breakup is discussed in the Appendix.

The second factor in eq. (2) arises from the integration over fragment momentum, which has a maxwellian distribution characterized by the ensemble temperature $\tau = 1/\beta$.

The third factor ζ_{AT} is the intrinsic partition function of the nuclear species AT:

$$\zeta_{AT} = \sum_i g_{AT}^{(i)} e^{-\epsilon_{AT}^{(i)}/\tau} \tag{3}$$

where $g^{(i)}_{AT} = 2j^{(i)}_{AT} + 1$ is the degeneracy of the energy level $\varepsilon^{(i)}_{AT}$ of the species AT. We have attempted to use the maximum available experimental information on the nuclear levels [6]. However, as the mass number A and the excitation energy ε increase, the data grow more and more scarce, first with regard to the degeneracies $g^{(i)}_{AT}$, later on for the level positions $\varepsilon^{(i)}_{AT}$ as well.

Therefore, we have found it necessary to develop a simple semi-empirical formula for the density of levels in light nuclei at high excitation. The functional form

$$\rho_{AT}(\varepsilon) = \frac{k_1}{A^{5/3}} e^{\sqrt{2a(A)\varepsilon}} \tag{4}$$

with the level density parameter given by

$$a(A) = \frac{A}{8\ \text{MeV}} \left(1 - \frac{k_2}{A^{1/3}}\right) \tag{5}$$

has been fitted to the available information on light nuclei, leading to $k_1 = 0.2$ and $k_2 = 0.8$. The calculated results are not critically sensitive to variations of these parameters.

The above formula (4) represents an estimate of the total level density in a given nuclear species. However, in the present context, we are interested in levels with a half-life longer than a specified time characterizing the duration of the explosion. Generally it is expected that the higher the excitation energy of a level, the shorter is its half-life. Unfortunately, we are faced with the fact that very little is known about the stability properties of highly excited levels in very light nuclei. Therefore, we have made the following simplistic ansatz for the density of sufficiently stable levels,

$$\rho^{eff}_{AT}(\varepsilon) = \rho_{AT}(\varepsilon)\, e^{-\frac{(\varepsilon-B)^2}{2\varepsilon^2_{cut}(A)}} \quad . \tag{6}$$

Here B is the barrier against the dominant decay mode of the nucleus AT (see later), while $\varepsilon_{cut}(A)$ is determined on the basis of the available data [6]. In our standard scenario, we wish to include all levels with a width less than one MeV, $\Gamma \leq 1$ MeV, corresponding to a half-life $T_{1/2} > 5 \cdot 10^{-22}$s. On the basis of ref. [6], we find that for nuclei with $5 \leq A \leq 16$ this can be achieved with the following approximation

$$\varepsilon_{cut} = c(A - 4) \tag{7}$$

with $c \approx 2$ MeV. The parameter c characterizes the extension of the explosion process in time and is in this way somewhat analogous to the volume parameter χ. These two parameters are the essential parameters of the model. Following the same guideline of including only levels with $\Gamma < 1$ MeV, we exclude the broad excited levels above 20.1 MeV in ^{4}He and also the dinucleon resonance. We shall examine the sensitivity of the calculated results to these levels.

Once specification has been made of the model parameters (namely the available energy per nucleon ε, the isospin asymmetry $I = (N - Z)/A$, and the parameters χ and c), the Lagrange multipliers β, μ, and ν are determined as in ref. [1] by solving the following three coupled constraint equations:

$$\begin{aligned} \varepsilon &= \sum_{AT} \left(\tfrac{3}{2}\tau + V_{AT} + \bar{\varepsilon}_{AT}\right)\omega_{AT} \\ 1 &= \sum_{AT} A\omega_{AT} \\ I &= \sum_{AT} 2T\omega_{AT} \quad . \end{aligned} \tag{8}$$

Here

$$\bar{\epsilon}_{AT} = \frac{1}{\xi_{AT}} \sum_i \epsilon_{AT}^{(i)} g_{AT}^{(i)} \, e^{-\beta \epsilon_{AT}^{(i)}} \tag{9}$$

is the average excitation energy of fragments of the species AT. Subsequently, the partition function Z in eq. (1) can be constructed, yielding all the statistical information on the system immediately after the explosion.

2.2. Evaporation

The description of the secondary evaporative stage of the process forms a special problem since ordinary evaporation theories are not reliable for highly excited, very light nuclei. Therefore, it has been necessary to develop a simple procedure for treating the sequential deexcitation of the many nuclear species under consideration.

At a given stage of the deexcitation process, the excited nucleus may decay by emission of either a nucleon or an alpha particle; the emission of other composite particles, such as deuterons, is neglected, since these processes are expected to be less favored. The dominant decay mode is determined on the basis of the estimated decay barriers given by

$$B = S + V \tag{10}$$

Here $S = M_{ejectile} + M_{residue} - M_{ejector}$ is the separation energy of the ejectile (with M denoting the experimental mass excess). The electrostatic contribution to the barrier is estimated by

$$V = \begin{cases} 0 & \text{for n} \\ V_p = \dfrac{(Z-1)e^2}{R+d_p} \;, \; d_p = 1.5 \text{ fm} & \text{for p} \\ V_\alpha = \dfrac{Z(Z-2)e^2}{R+d_\alpha} \;, \; d_\alpha = 0.5 \text{ fm} & \text{for } \alpha \end{cases} \tag{11}$$

where $R = r_o A^{1/3}$ is the nuclear radius, with $r_o = 1.15$ fm. Although the constants r_o, d_p, and d_α are somewhat uncertain, the above procedure predicts the correct dominant decay modes for the nuclei under consideration. For example, among the nuclei up to A = 12, alpha decay is the dominant decay mode for ^{6}Li, ^{7}Li, ^{7}Be, ^{8}Be, ^{10}B, ^{12}C.

If nucleon decay is dominant, the branching between neutron and proton evaporation is considered. When alpha decay is dominant, only this mode is included. The excitation spectrum of the nuclei emerging from the explosion is characterized by the ensemble temperature $\tau = 1/\beta$, so the population of a given level with energy $\varepsilon_{AT}^{(i)}$ is given by

$$f_{AT}^{0}(\varepsilon_{AT}^{(i)}) \sim g_{AT}^{(i)}\, e^{-\varepsilon_{AT}^{(i)}/\tau} \tag{12}$$

The subsequent evaporation stage modifies this distribution. It is easy to solve the sequential evaporation problem recursively, starting from the heaviest nucleides included. A given nucleus then receives contributions to its population from the various types of decay from heavier nuclei, so its energy distribution prior to its own decay is given by

$$f_{AT}(\varepsilon_{AT}^{(i)}) = f_{AT}^{o}(\varepsilon_{AT}^{(i)}) + \sum{}' \sum_{k} (\varepsilon'_{max} - \varepsilon_{AT}^{(i)})\, g_{AT}^{(i)} f_{AT}(\varepsilon_{A'T'}^{(k)}) \tag{13}$$

where the primed sum extends over the three types of decay process considered (i.e., n, p, and α decay) and A'T' denotes the respective emitter nucleide. Furthermore, k enumerates the nuclear levels in the emitter and $\varepsilon'_{max} = \varepsilon_{A'T'}^{k} - S$ is the maximum kinetic energy of the ejectile. The energy factor arises from the integration over the momentum of the ejectile n, p, or α. It is understood that only levels with a positive value of ε'_{max} decay - the others are particle stable and will eventually decay to the ground state by gamma emission. This method of solving the cascade problem yields the final populations in a rather easy and convenient way.

3. Results

The model described above has been employed for calculating the intensive quantities characterizing the disassembly of a hot, and sufficiently large, piece of nuclear matter. The first, fast stage of the disassembly process (the explosion) produces a distribution of fragments that, at least at the one-particle inclusive level, can be described statistically. Figure 1 shows the ensemble temperature τ and the specific entropy σ characterizing this stage of the process, as functions of the available excitation energy per baryon ϵ. Two extreme values of the volume parameter χ have been considered: $\chi = 1$ (solid curves) and $\chi = 3$ (dashed curves); we expect the physically relevant values of χ to lie between those two extremes, cf. Appendix. The calculated curves are insensitive to the actual value of the isospin asymmetry variable $I = (N - Z)/A$. Figure 1a also includes the curve corresponding to an ideal gas of free nucleons: $\tau = \frac{2}{3}\epsilon$ (dot-dashed curve). Production of composite fragments effectively reduces the number of translational degrees of freedom and thereby raises the temperature. This effect is most pronounced at lower energies and for small values of the volume parameter χ. At higher energies pion production begins to play a role, providing an efficient mechanism for cooling the system below the ideal gas temperature. In fig. 1b we include results from other calculations [7-9]. It can be seen that our results for the pre-evaporation stage (in particular for $\chi = 1$) agree reasonably well with those of other models. However, since the subsequent evaporation stage can lead to observable quantities rather different from those associated with the explosion, the original statistical quantities lose their significance.

In order to demonstrate the importance of the evaporation in shaping the final distributions, we compare in fig. 2 the relative yields of final

fragments (solid histogram) with those associated with the pre-evaporation stage (dashed histogram), in one particular example having ϵ = 20 MeV, χ = 1, and I = (N-Z)/A = 0. The most spectacular difference is, of course, that all the A = 5 nuclei disappear in the final distribution. Furthermore, the yield of alpha particles is increased by about a factor of six and actually becomes a local maximum in the distribution. A similar effect is found for other especially stable nuclei. The number of free nucleons is also increased significantly (more than 30% in the present example), while the deuterons receive only a relatively small contribution from the evaporation. On the other hand, the heavy species tend to suffer substantial losses, particularly so for the less stable odd-A nucleides. This change of the relative abundancies of the various fragment species significantly affects the final deuteron-to-proton yield ratio, d/p. This general feature makes it essential to take account of the decay of composite fragments if one attempts to use d/p as a measure of the entropy of the initial source. Such an idea was introduced in ref. [7] and has also been discussed in refs. [10,11].

The formation of unbound nucleides during the explosion stage also has the appealing effect of enhancing the final abundancies of particularly stable species, such as ^{4}He. Figure 3 shows a comparison of our results for relative fragment yields (solid histogram) to those of an earlier calculation where only particle-stable nuclear states have been included in the statistical explosion (dashed histogram) [1]. The parameter values are the same as in fig. 2. While the dashed histogram does not exhibit maxima for the more stable nuclei (in fact, odd-A species are sometimes more abundant than the neighboring even ones), nuclei with A = 4,12 (and to a lesser extent A = 6,8,10) show pronounced peaks in the present calculation. This inversion arises mainly because well-bound stable nuclei usually tend to have fewer particle-stable excited levels than those with less bound ground states.

Now we wish to establish contact between our calculated results and experimental data. Since only intensive quantities appear in eq. (8), the results apply to all systems with the same values of ε and I. The corresponding extensive quantities (i.e., the absolute production cross section σ_{AT} of a given fragment species AT) scale with the source size A_o. In fact, σ_{AT} is of the form

$$\sigma_{AT} = \sigma_o \, A_o \, \omega_{AT} \tag{14}$$

where σ_o is the cross section for forming a source and A_o is the average number of nucleons in the source. The source is identified with the participant nucleons and is assumed to be composed of nucleons from the projectile and target according to the standard sharp-sphere clean-cut geometry; this leads to [12]

$$A_o = \frac{A_T A_P^{2/3} + A_P A_T^{2/3}}{(A_P^{1/3} + A_T^{1/3})^2} \quad . \tag{15}$$

Using the geometric reaction cross section $\sigma_o = \pi r_o^2 (A_P^{1/3} + A_T^{1/3})^2$ and (15) we obtain

$$\sigma_{AT} = \pi r_o^2 [A_T A_P^{2/3} + A_P A_T^{2/3}] \, \omega_{AT} \quad . \tag{16}$$

Figure 4 displays the absolute cross section for protons, σ_p, as a function of the quantity $A_T A_P^{2/3} + A_P A_T^{2/3}$ for nuclear collisions with $E_{beam}/A = 800$ MeV. The curves represent expected limits of the parameter range. The data are taken from ref. [12]. It is seen that the predicted linear dependence is borne out and that the absolute sizes are in good mutual agreement.

In subsequent figures we plot relative yield ratios for different fragment species as functions of the available energy ε. In order to make a

comparison with the data, it is necessary to calculate the values of ϵ appropriate to the different reactions investigated experimentally [12]. Since the identification of the source with the participant nucleons led to a good description of the absolute cross sections, we use the same ideas to estmate the available energy. Thus, we assume that the kinetic energy of the participant nucleons is available for the explosion. It should be noted, though, that specific dynamical models may yield different distributions of the energy; e.g., in a hydrodynamical picture approximately half the total energy is contained in the macroscopic flow of matter and only the remainder is available for statistical excitation [13].

Figure 5 shows the d/p ratio obtained for several values of the model parameters, as a function of the available energy per participant nucleon, ϵ. Unless otherwise indicated, the lower boundary of the different bands on the figures represents symmetric systems ($I = \frac{N-Z}{A} = 0$), while the upper boundary corresponds to the value $I = 0.2$, which characterizes the combined system C + Pb and is the highest value of relevance. Figure 5a shows the results of the model for two limiting values of the volume parameter, $\chi = 1$ (solid curves) and $\chi = 3$ (dashed curves), with the life-time parameter in eq. (7) held constant at $c = 2$. In fig. 5b the volume parameter is kept constant at $\chi = 1$ and the number of levels included is varied. The results displayed have been calculated with $c = 1$ (dashed curve), $c = 2$ (solid curves), and $c = 4$ (dot-dashed curves). The calculations displayed in figs. 5a,b have included only the "standard" levels for $A \leqslant 4$, i.e., the only excited state for $A \leqslant 4$ is the level at $\epsilon = 20.1$ MeV in ^{4}He. In fig. 5c the standard value $c = 2$ has been kept, but we have included either the dinucleon resonance at around 2.2 MeV (dashes) or the broad excited levels in the alpha particle above 20.1 MeV (dot-dashes). The data points have been included in these figures.

Figure 5 demonstrates that the relative yields are rather sensitive to the value of the volume parameter χ but (at least at higher energies) not too sensitive to moderate variations in the parameter c. On the other hand, the role of the dinucleon resonance is significant, while the broad excited states in the alpha particle affect the results only moderately. The width of the dinucleon resonance can be estimated from free nucleon-nucleon scattering phase shifts at low energies. Using $\Gamma \approx 2\varepsilon/\delta$ with $\varepsilon \approx 2$ MeV and $\delta \approx 1$ for the phase shift [3] we arrive at the estimate $\Gamma \approx 4$ MeV. This corresponds to a lifetime not much shorter than our rough estimate of the time scale for the explosion phase. Hence a specific dynamical model is probably required to determine whether the dinucleon should be included in the explosion or not. One might also argue conversely: if it is possible to fix the other parameters, the present model may offer a tool for learning about the time scale of the disassembly process, insofar as the calculated results are sensitive to the inclusion of a particular state with a known lifetime.

In the subsequent figures we consider the standard scenario: c = 2 and only the 20.1 MeV excited state in ^{4}He included for $A \leqslant 4$. Figure 6 displays the alpha-to-proton yield ratio, α/p, for two different values of the volume parameter: $\chi = 1$ (solid curves) and $\chi = 3$ (dashed curves). As indicated by fig. 2 and recent calculations [14], the alpha yield seems to provide the most sensitive test of the theory of the disassembly of nuclear matter. Ref. [14] discusses the possibility of a Bose condensation of alpha particles, in analogy to what has been predicted earlier for low-energy pions [15]. In view of this, it is unfortunate that only relatively few measurements of the alpha yield have been reported in ref. [12], and more measurements of the alpha yields in medium-energy nuclear collisions would be highly desirable.

Figure 7 is an illustration of our results for the relative yields of other fragments. Figure 7a shows the ^{3}He/p yield ratio, while fig. 7b displays the triton-to-proton yield ratio, t/p. As in fig. 5, one observes a remarkable trend of constancy in the gross structure of the experimental data as a function of ϵ, which the model does not reproduce, particularly for the lower energies, $\epsilon < 100$ MeV. This discrepancy may be partly attributed to the fact that classical statistics has been used, although quantum statistics play an important role at energies below the Fermi energy, as pointed out, e.g. in [14]. Nevertheless, more experimental data are necessary (particularly in the ranges 20 MeV $< \epsilon <$ 80 MeV and 100 MeV $< \epsilon <$ 150 MeV) in order to allow definite conclusions about the model.

In fig. 8 we compare the prediction of our model for the yield ratio of positive and negative pions to protons, and compare with data [12]. The calculations have been carried out for two different values of the volume parameter: $\chi = 1$ (solid curves) and $\chi = 3$ (dashed curves). It can be seen that pion production sets in with about the same slope in theory and experiment, but the calculation overestimates the absolute pion yields significantly. This may not be surprising in view of the experimental finding [16] that the pion multiplicities scale with a power close to 2/3 of the source size A_o. This suggests that pion production may be mainly associated with the surface of the system, and the present model would have to be refined accordingly before good agreement for the pions could be expected.

It is instructive to note the neutron-to-proton yield ratio, n/p, as a function of ϵ. This quantity is shown in fig. 9a. The results do not depend strongly on χ, but they are sensitive to the neutron excess in the source, I. For neutron-rich systems the presence of composite nucleides amplifies the resulting ratio between free neutrons and protons, as has been discussed in

[1]. This effect persists in the ratio between ^3H and ^3He (fig. 9b), where we can compare our results to the data points of ref. [12]. It is seen that the symmetric systems have $^3H/^3He$ slightly larger than unity both in the data and in the calculation. Experimental points representing the more asymmetric systems fall in a region around the theoretical curves labeled by $I = 0.2$. Figure 9c displays the ratio between negative and positive pions as a function of ε, with the data from ref. [12] included. While the data points are generally contained within the calculated range, their energy dependence appears to be somewhat weaker.

As mentioned in Section 2, in the calculations we have neglected the fragment-fragment interactions that are dominated by the electrostatic repulsion. Due to the long range of the Coulomb force, this contribution can be approximated by assuming that the fragmentation occurs in a configuration-independent electrostatic potential ϕ (identified with half the typical electric potential inside the source) [1]. The potential energy of a given species is then increased by the amount $Z_o e\phi$, where Z_o is the charge of the source. On the basis of this mean-field approximation it can be shown that the calculated results depend only slightly on the Coulomb parameter ϕ: furthermore, the main effect is an effective decrease of the available excitation energy ε by the amount $\frac{Z_o}{A_o}\phi$. This feature is reflected in slightly lower temperatures and entropies; the yield of pions and light nuclei is correspondingly somewhat smaller, and the yield of heavier fragments slightly larger, than with $\phi = 0$. This effect is less than a few percent in all quantities.

4. Concluding remarks

The present study is relevant for nuclear collisions at intermediate energies, say from 20 to 200 MeV per nucleon. The apparent lack of small parameters, on which the physics discussion can be based, constitutes a particular challenge of medium-energy nuclear physics. This situation is in contrast to low-energy nuclear reactions, where the smallness of the macroscopic velocities relative to the intrinsic nucleonic motion has a number of simplifying consequences and to high-energy nuclear collisions where the largeness of the bombarding energy on the nucleonic scale allows some important approximations.

In the present paper we have studied the disassembly of a hot nuclear system in a two-stage idealization. In the first stage the system quickly explodes into many excited nuclear fragments. While conceptually similar to the approach in ref. [1], the present description of the explosion is more general in that also particle unstable nuclear levels are considered accessible. Therefore, a subsequent evaporative stage need be considered during which the unstable fragments deexcite.

We have demonstrated that the inclusion of unstable levels does in fact affect the final, observable fragment abundancies significantly. Therefore, this inclusion appears necessary in any quantitative model. An example of special current interest is the deuteron-to-proton yield ratio. It was shown that the decay of unstable heavier fragments contributes a substantial number of debris protons, particularly at lower bombarding energies, so the observable d/p ratio emerges as relatively independent of energy, a feature that is clearly indicated by the data but that can not be reproduced in statistical models neglecting unstable fragments.

Other fragment yield ratios have also been compared with data. The calculations exhibit an encouraging degree of agreement with the data, although they yield a somewhat stronger beam energy dependence than is indicated by the data. However, considerably more data are necessary before any firm conclusions can be drawn.

Until now, our attention has focused on the fragment yields. However, the differential angular distributions and energy spectra can readily be calculated in the model, although some additional practical work would be required. If the further confrontation with more complete data proves successful, the differential quantities should be considered subsequently. While p, d, and t spectra from relativistic nuclear collisions have already been measured [17], there is a great need for additional data, in particular for heavier fragments.

The present work focuses on one particular aspect of medium-energy nuclear collisions, namely the disassembly into observable fragments at the final stages of the collision process. This aspect has so far been largely ignored in existing dynamical collision models, such as nuclear fluid dynamics and intra-nuclear cascades, which yield only an unstructured matter distribution emerging from the reaction zone. An important next step would therefore be to augment the dynamical models with the present model for the disassembly phase. Such efforts are presently under way [18], and we hope they will lead to a more complete description of the entire collision process.

In the course of this work we have had stimulating discussions with S.E. Koonin, H. Stöcker, and W.J. Swiatecki. This work was supported by the Director, Office of Energy Research, Division of Nuclear Physics of the Office of High Energy and Nuclear Physics of the U.S. Department of Energy under Contract W-7405-ENG-48.

Appendix: The relation between χ and ρ

In the following discussion, we ignore the isospin variable T and assume that a nuclear species is characterized by its mass number A alone; this simplification is merely for notational convenience.

Each term in the partition function Z refers to a definite fragmentation channel characterized by the numbers $\{n_A\}$ with n_A denoting the number of fragments with mass number A. The total number of fragments in that particular channel is given by $N = \sum_A n_A$.

The position of a fragment is denoted by $\vec{r}_{i_A}^{(A)}$ where $i_A = 1,\ldots n_A$ enumerates the n_A fragments of the species A. The contribution to the partition function from the integration over the fragment positions is of the form

$$\int d\vec{r}_1^{(1)} \int d\vec{r}_2^{(1)} \ldots \int d\vec{r}_{n_1}^{(1)} \int d\vec{r}_1^{(2)} \ldots \int d\vec{r}_{n_2}^{(2)} \ldots = \prod_{A=1}^{\infty} \prod_{i_A=1}^{n_A} \int d\vec{r}_{i_A}^{(A)} \qquad (A\text{-}1)$$

A rough estimate of this N-dimensional volume integral is the N^{th} power of some volume characterizing the size of the system. As a convenient reference volume we use $\frac{4\pi}{3} r_o^3 A_o$ where A_o is the (average) total number of nucleons in the system. However, the quantitative evaluation is complicated by the circumstance that in general the different position coordinates are not independent of each other. This is so because each fragment occupies a certain volume in space and thereby makes that domain inaccessible to other fragments. In order not to introduce complications beyond the scope of the model, we have introduced the parameter χ by writing the above integral eq. (A-1) as

$$(\chi \frac{4\pi}{3} r_o^3 A_o)^N \quad . \qquad (A\text{-}2)$$

This is equivalent to assuming that the average available volume for any fragment amounts to

$$\left\langle \int d\vec{r}_i^{(A)} \right\rangle_A = \chi \frac{4\pi}{3} r_o^3 A_o \quad . \tag{A-3}$$

In order to make contact with other models, it is necessary to relate χ to the physical break-up density of baryons. To this end we analyze the relatively simple case where only fragments of the same size occur. This case presents a good illustration since equipartition is actually the most probable fragmentation for channels with a given number of fragments.

Consider then a volume V in which N equal fragments are present. Let each of them block a volume V_o/N, where $V_o < V$. We shall study the thermodynamic limit where $V, V_o, N \to \infty$ while V_o/V remains constant. The N coupled volume integrals in (A-1) can then be evaluated by first performing an unrestricted integration over (any) one of the position variables, then integrating over another one with the restriction that it not enter the domain blocked by the first one, and so on. This procedure leads to the result

$$\prod_{i=1}^{N} \int d\vec{r}_i = V\left(V - \frac{V_o}{N}\right)\left(V - 2\frac{V_o}{N}\right)\cdots\left[V - (N-1)\frac{V_o}{N}\right] \quad . \tag{A-4}$$

After some algebraic manipulation, the use of Stirling's formula results in the form

$$\prod_{i=1}^{N} \int d\vec{r}_i \approx \left[\frac{V}{e}\left(1 - \frac{V_o}{V}\right)^{1 - \frac{V}{V_o} - \frac{1}{2N}}\right]^N \quad . \tag{A-5}$$

On the other hand, from the definition (A-3) of χ we also have

$$\prod_{i=1}^{N} \int d\vec{r}_i = (\chi V_o)^N \quad . \tag{A-6}$$

Therefore, by identification, we find

$$\chi \approx \frac{V}{V_o} \frac{1}{e} \left(1 - \frac{V_o}{V}\right)^{1 - \frac{V}{V_o}} \qquad \text{(A-7)}$$

where the term 1/2N in the exponent has been neglected, as is justified in the limit $N \to \infty$.

Two interesting cases are the dense limit ($V_o \approx V$) and the dilute limit ($V_o << V$). In the dense limit $V_o \to V$ we have $1 - V/V_o = \varepsilon \to 0$ and hence

$$\chi \to \frac{1}{e} \approx 0.37 \qquad \left(\frac{V_o}{V} \to 1\right) . \qquad \text{(A-8)}$$

In the dilute limit we have to leading order in the small quantity V_o/V

$$\chi \approx \frac{V}{V_o} - \frac{1}{2} \approx \frac{V}{V_o} \qquad \left(\frac{V_o}{V} \to 0\right) . \qquad \text{(A-9)}$$

A numerical comparison of χ in (A-7) and the above dilute-limit formula (A-9) shows that the latter actually provides a very good approximation up to values of V_o/V rather close to unity, say up to $V_o/V \approx 0.8$.

The relation between χ and the nucleon density ρ can be established by assuming that the volume blocked by a given fragment with mass number A is simply equal to the standard nuclear volume $\frac{4\pi}{3} r_o^3 A$. The average nucleon density in the considered volume V is then given by $\rho = \frac{V_o}{V} \rho_o$ where $\rho_o = \left(\frac{4\pi}{3} r_o^3\right)^{-1}$ is the nucleon density in standard nuclear matter. By inserting this relation into the general expression (A-7), or its approximate form (A-9), one obtains a useful correspondence between the volume parameter χ and the standard break-up density ρ. In particular, it follows that the values $\chi = 1$ and 3 correspond to $\rho \approx 0.7 \rho_o$ and $0.3\ \rho_o$, respectively. We expect that these two values provide brackets on the break-up density.

References

1. J. Randrup and S.E. Koonin, Nucl. Phys. A356 (1981) 223.
2. E. Fermi, Prog. Theor. Phys. 5 (1950) 570.
3. A. Mekjian, Phys. Rev. C17 (1978) 1051.
4. J. Gosset, J.I. Kapusta and G.D. Westfall, Phys. Rev. C18 (1978) 844.
5. P. Bond, P.I. Johansen, S.E. Koonin and S. Garpman, Phys. Lett. 71B (1977) 43.
6. Table of Isotopes, ed. C.M. Lederer and V.S. Shirley (Wiley, N.Y. 1978).
7. P.J. Siemens and J.I. Kapusta, Phys. Rev. Lett. 43 (1979) 1486.
8. I.N. Mishustin, F. Myhrer and P.J. Siemens, Phys. Lett. 95B (1980) 361.
9. H. Stöcker, J.A. Maruhn and W. Greiner, Phys. Lett. 81B (1979) 303.
10. G. Bertsch and J. Cugnon, preprint (1981).
11. H. Stöcker, preprint LBL-12302 (1981).
12. S. Nagamiya, M.-C. Lemaire, E. Moeller, S. Schnetzer, G. Shapiro, H. Steiner and I. Tanihata, Phys. Rev. C24 (1981) 971.
13. P.J. Siemens and J.O. Rasmussen, Phys. Rev. Lett. 42 (1979) 880.
14. P.R. Subramanian, L.P. Csernai, H. Stöcker, K.A. Maruhn, W. Greiner and H. Kruse, J. Phys. G., in press.
15. J. Zimányi, G. Fái and B. Jakobsson, Phys. Rev. Lett. 43 (1979) 1705.
16. S. Nagamiya in Proceedings of the Fifth High Energy Heavy Ion Study, Berkeley (1981) and preprint LBL-12950.
17. A. Sandoval, H.H. Gutbrod, W.G. Meyer, R. Stock, Ch. Lukner, A.M. Poskanzer, J. Gosset, J.-C. Jourdain, C.H. King G. King, N.V. Sen, G.D. Westfall and K.L. Wolf, Phys. Rev. C21 (1980) 1321.
18. G. Fái, J. Randrup and H. Stöcker, preprint LBL-13358, in preparation.

Figure Captions

Fig. 1. The temperature τ(a) and the specific entropy σ(b) immediately after the explosion as functions of the available excitation energy per baryon ϵ, for two values of the volume parameter: $\chi = 1$ (solid curves) and $\chi = 3$ (dashed curves). In Fig. 1a light lines display the results without inclusion of pions, while heavy lines represent the full calculation. The curve corresponding to an ideal gas of free nucleons (dot-dashes) has also been included. Figure 1b includes results from other theoretical calculations; the sources of these curves are refs. 7, 8 and 9.

Fig. 2. Relative yields of final fragments (solid histogram) compared to those prior to the evaporation stage (dashed histogram) for the parameter values $\epsilon = 20$ MeV, $\chi = 1$, $I = (N-Z)/A = 0$.

Fig. 3. Comparison of the final relative fragment yields of the present model, which takes all nuclear levels with a width $\Gamma < 1$ MeV into account (solid heavy histogram), with those of an earlier calculation [1] where only stable ($\Gamma = 0$) nuclear levels have been included in the available phase space (dashed light histogram), for the parameter values $\epsilon = 20$ MeV, $\chi = 1$, $I = 0$.

Fig. 4. Absolute cross section for protons σ_p as a function of the quantity $A_T A_P^{2/3} + A_P A_T^{2/3}$ for nuclear collisions $E_{beam}/A = 800$ MeV. The curves represent expected limits of the parameter range. The experimental data (here and in all subsequent figures) are taken from ref. [12]. For each of the five different projectile-target combinations, the value of the isospin asymmetry I is given for the total system as well as for the average source.

Fig. 5. Deuteron-to-proton yield ratio (d/p) as a function of the available excitation energy per participant nucleon ϵ obtained for several values of the model parameters. The lower boundary of the different bands represents symmetric systems, while the upper boundary corresponds to $I = (N-Z)/A = 0.2$. The different sections of the figure show the dependence of d/p on (a) the volume parameter χ, (b) the life-time parameter c for nuclei $A \geqslant 5$, and (c) the excited states in nuclei $A \leqslant 4$.

Fig. 6. Alpha-to-proton yield ratio (α/p) as a function of the available energy per participant nucleon ϵ for two different values of the volume parameter: $\chi = 1$ (solid curves), $\chi = 3$ (dashed curves). The lower and upper boundaries of the different bands correspond to $I = 0$ and $I = 0.2$, respectively.

Fig. 7. ^{3}He-to-proton yield ratio (a) and triton-to-proton yield ratio (b) as functions of the available energy per participant nucleon ϵ for two different values of the volume parameter: $\chi = 1$ (solid curves and $\chi = 3$ (dashed curves). The lower and upper boundaries of the different bands correspond to $I = 0$ and $I = 0.2$, respectively.

Fig. 8. Pion-to-proton yield ratios for (a) positive pions and (b) negative pions, as functions of the available energy per participant nucleon ϵ, for the values $\chi = 1$ (solid curves) and $\chi = 3$ (dashed curves) of the volume parameter.

Fig. 9. Relative yield ratios of fragments with the same mass but different isospin component: (a) neutron-to-proton, (b) triton-to-^{3}He, (c) π^--to-π^+ as a function of the available energy per participant nucleon ϵ, for different values of the volume parameter χ and the isospin asymmetry I.

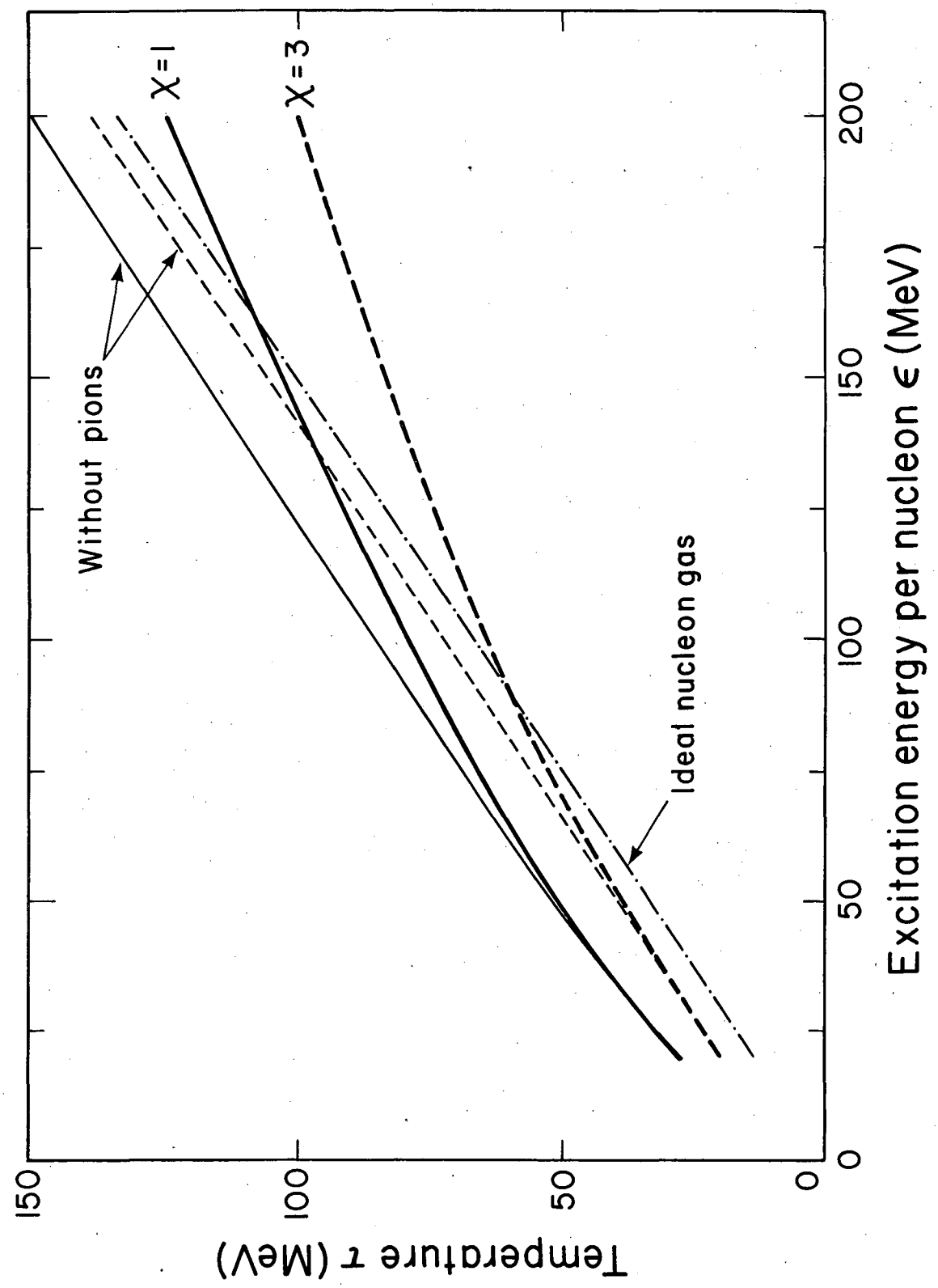

XBL 8110-1439

Fig. 1a

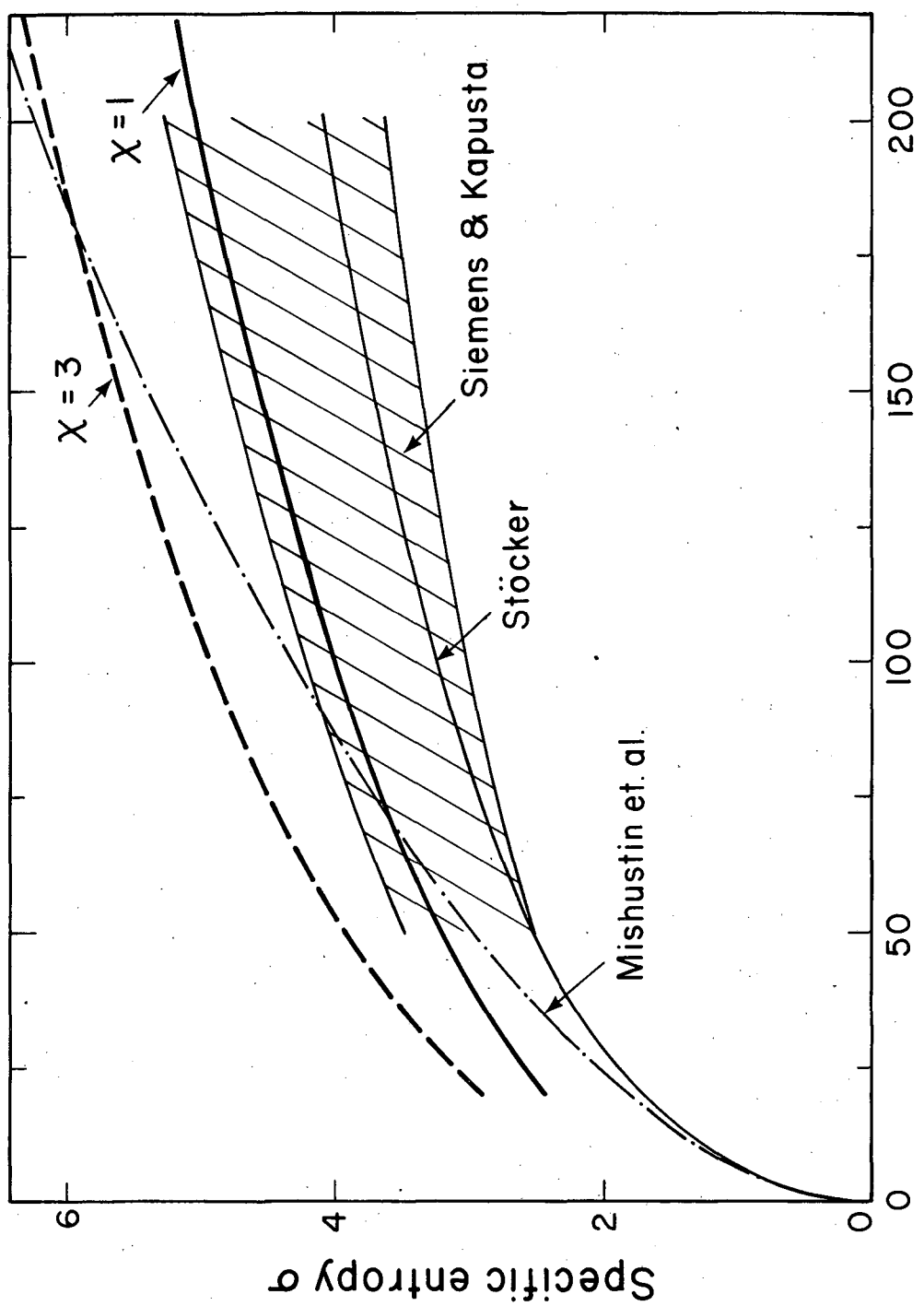

XBL 8110-1446

Fig. 1b

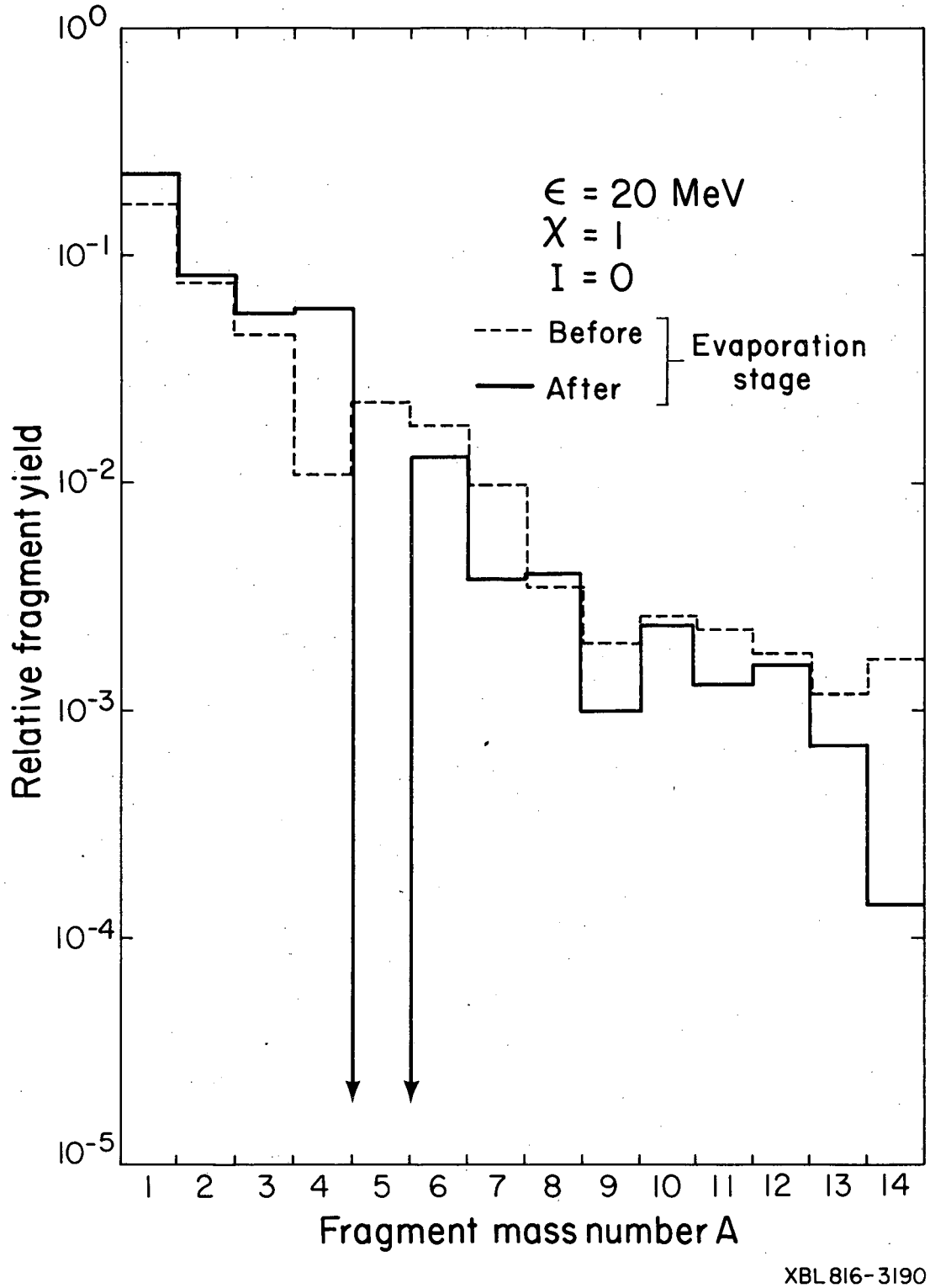
10^0
10^{-1}
10^{-2}
10^{-3}
10^{-4}
10^{-5}
Relative fragment yield
ϵ = 20 MeV
χ = 1
I = 0
---- Before
— After
Evaporation stage
1 2 3 4 5 6 7 8 9 10 11 12 13 14
Fragment mass number A
XBL 816-3190

Fig. 2

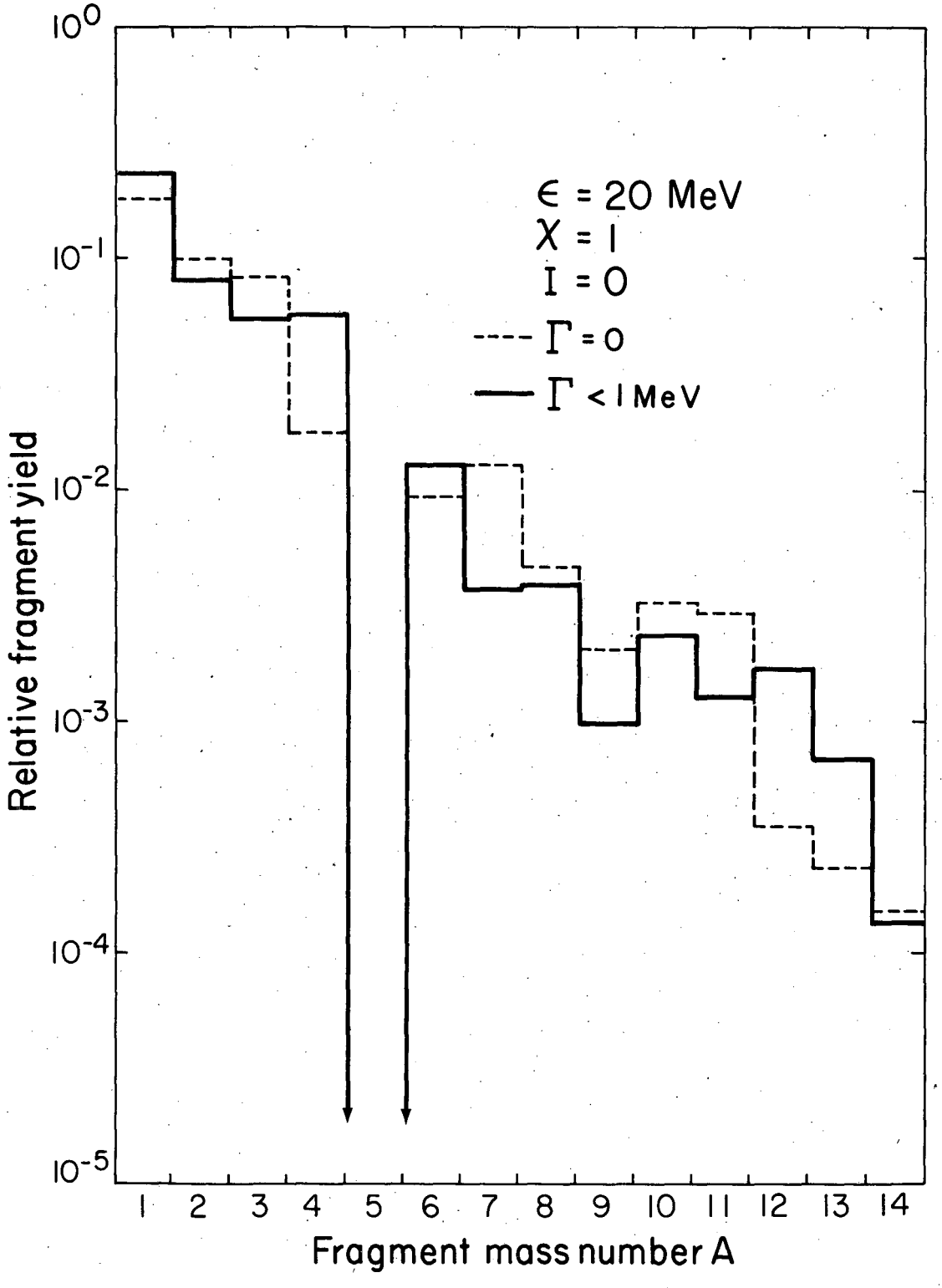

XBL 8110-1437

Fig. 3

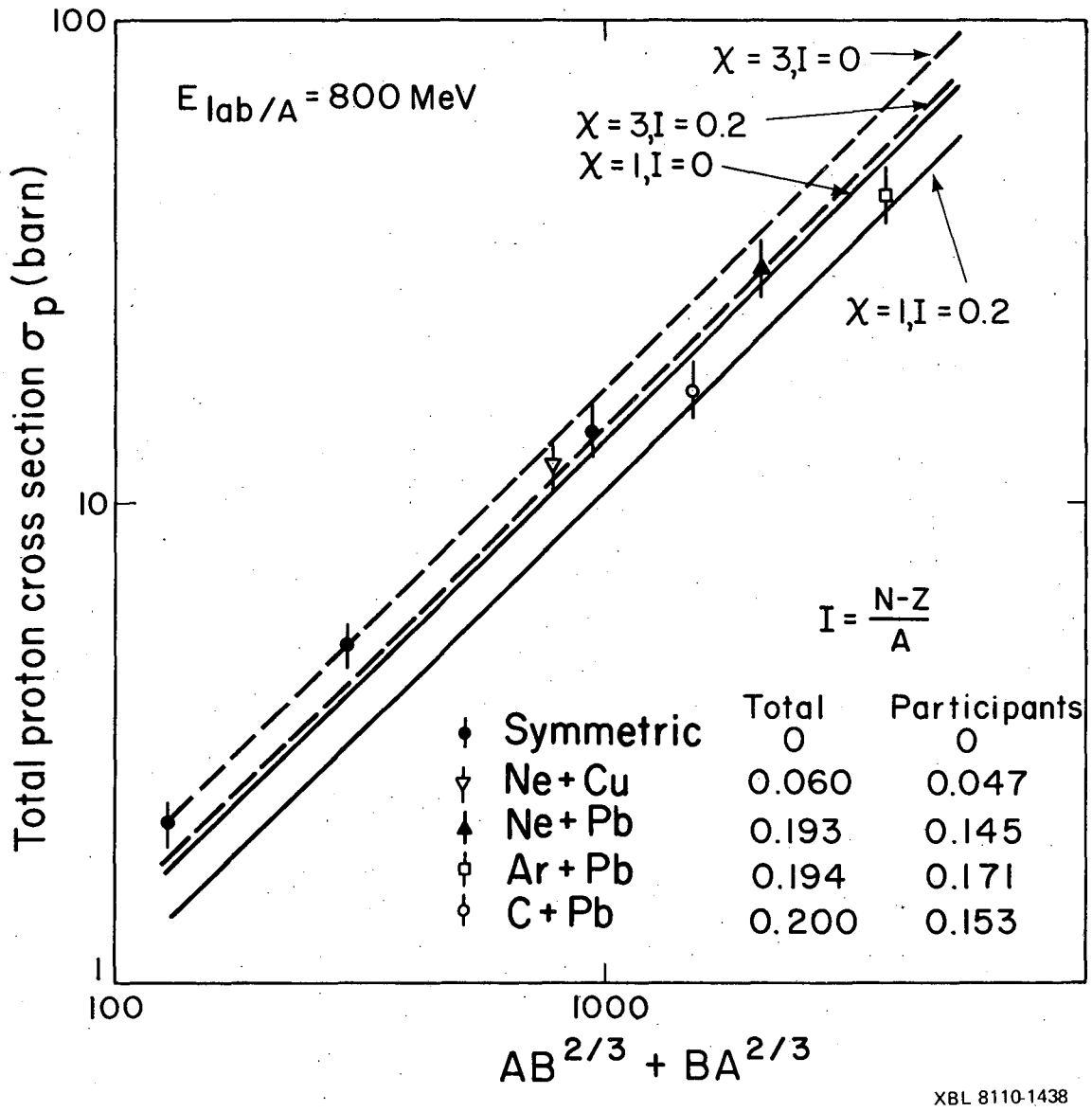
100
10
1
100
1000
$E_{lab/A}$ = 800 MeV
χ = 3,I = 0
χ = 3,I = 0.2
χ = 1,I = 0
χ = 1,I = 0.2
$I = \frac{N-Z}{A}$
Total proton cross section σ_p (barn)
$AB^{2/3} + BA^{2/3}$
Total
Participants
Symmetric 0 0
Ne + Cu 0.060 0.047
Ne + Pb 0.193 0.145
Ar + Pb 0.194 0.171
C + Pb 0.200 0.153
XBL 8110-1438

Fig. 4

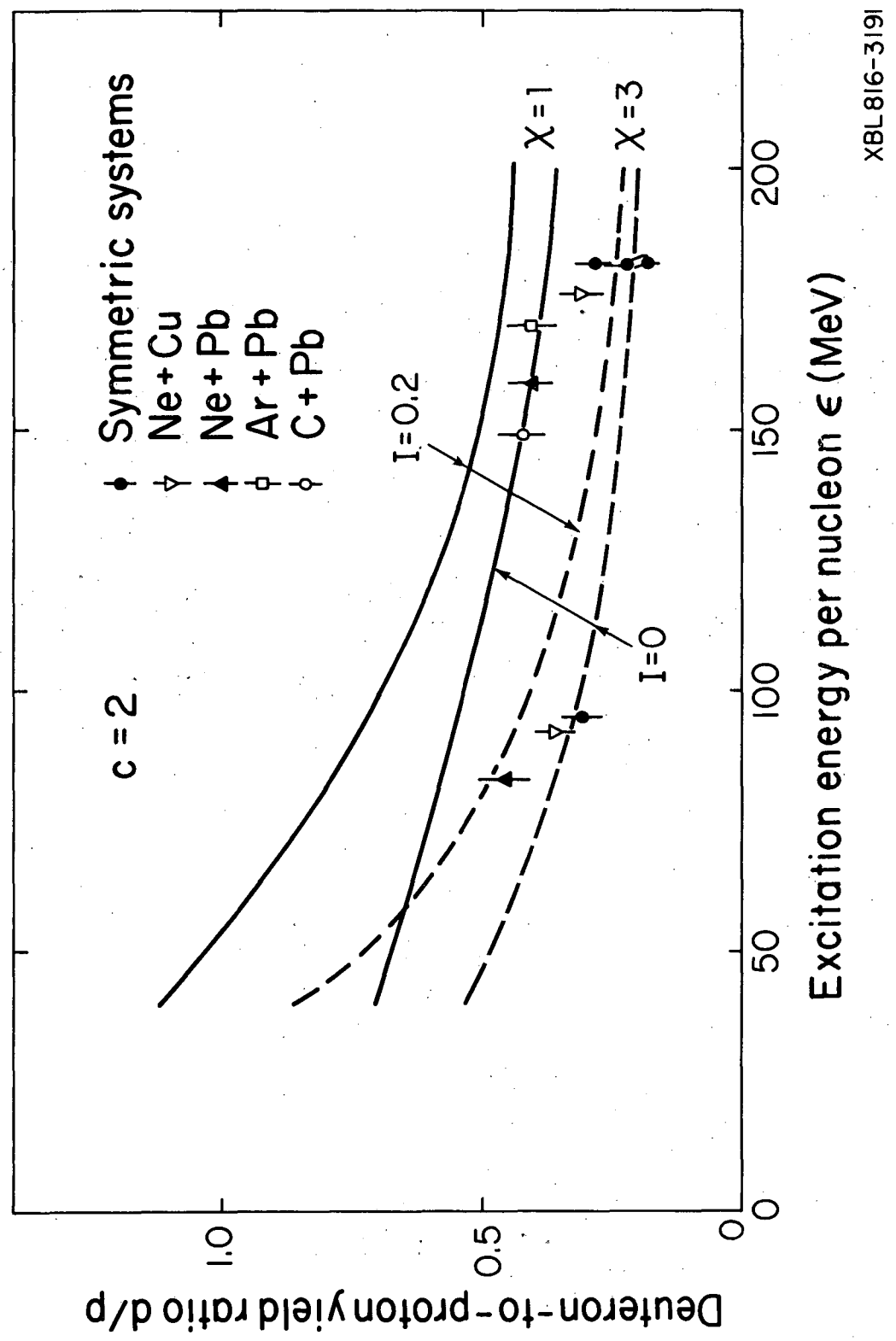

XBL816-3191

Fig. 5a

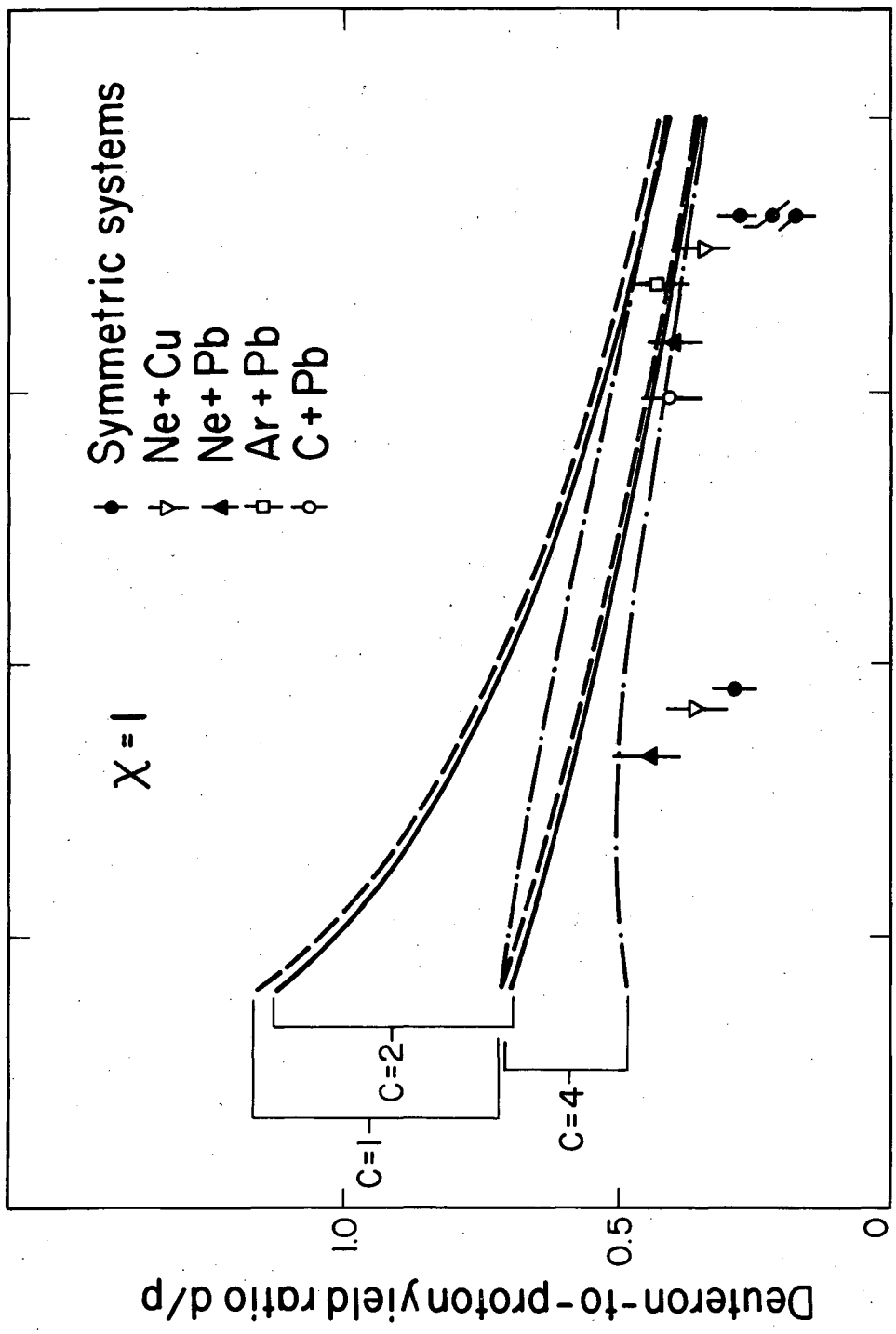

XBL 8110-1448

Fig. 5b

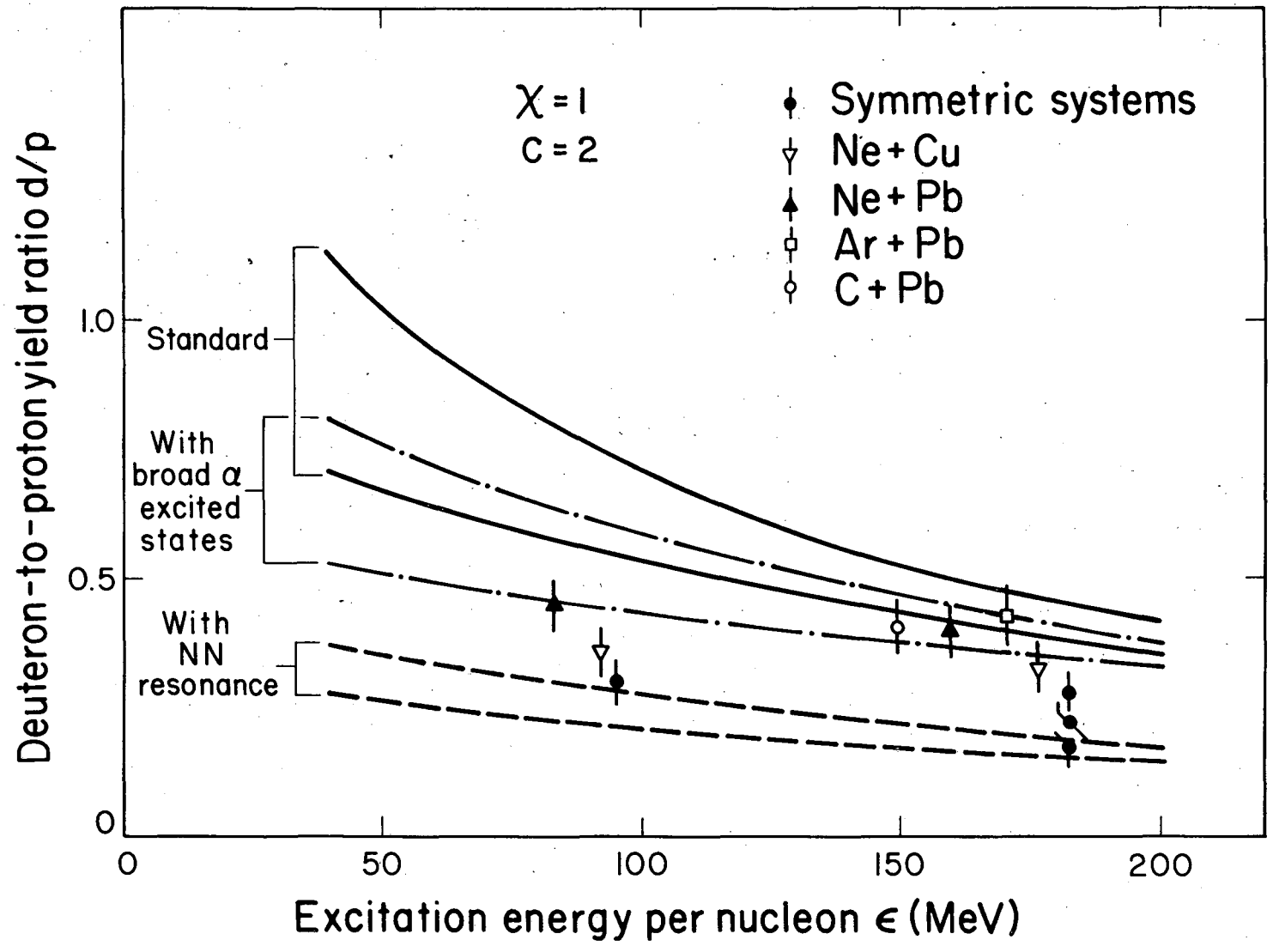

XBL 8110-1447

Fig. 5c

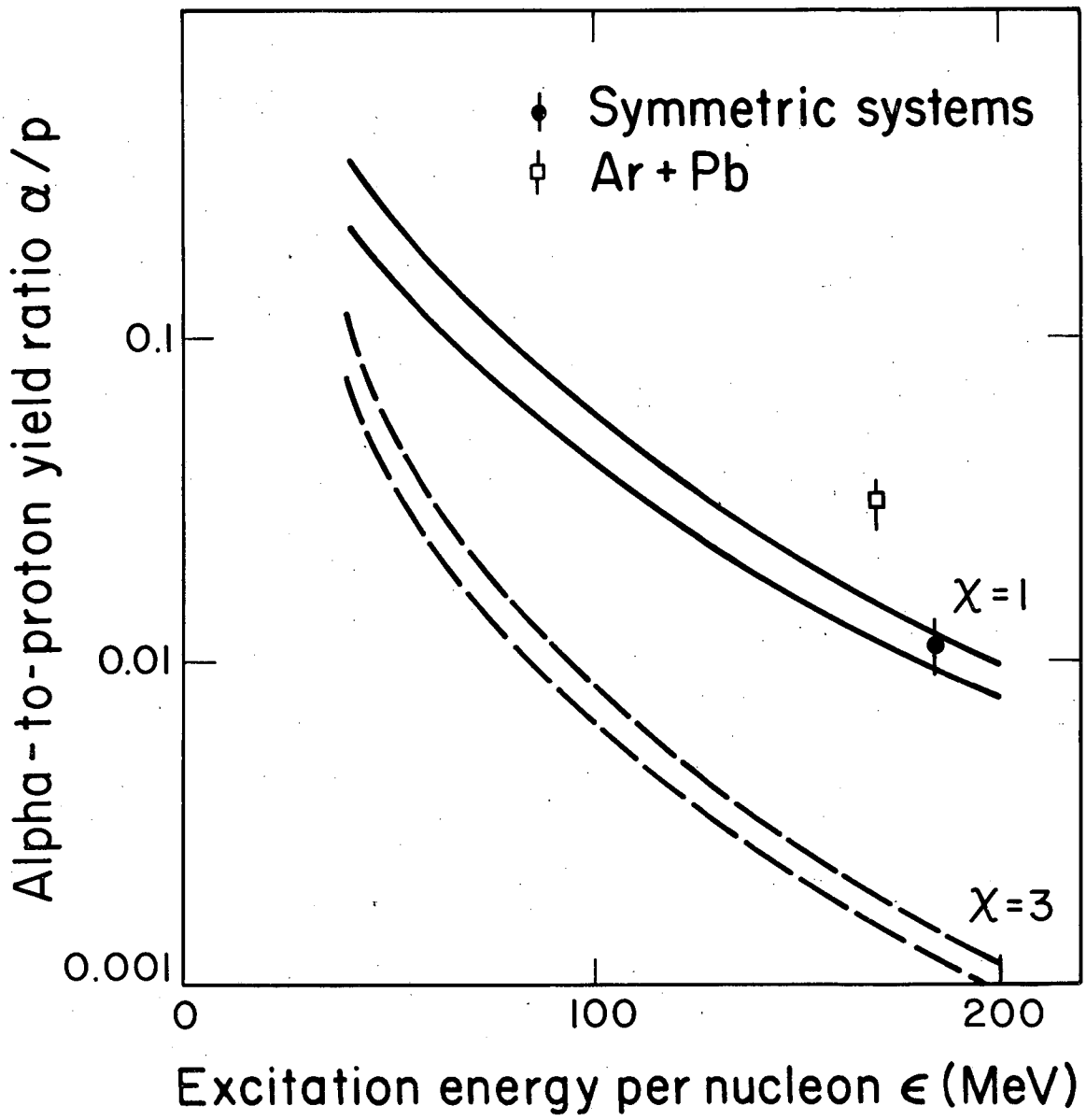

XBL 8110-1445

Fig. 6

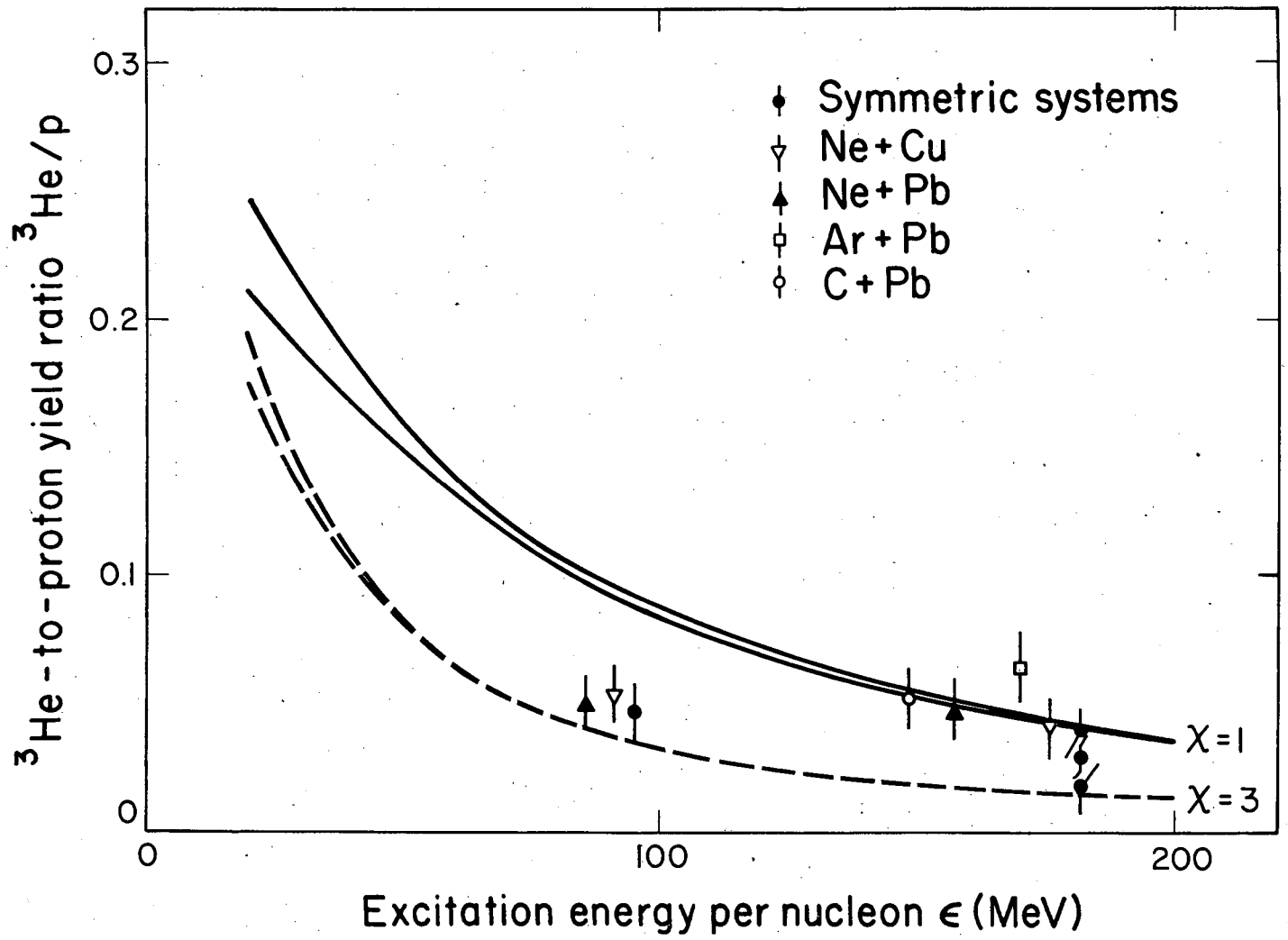

XBL 8110-1442

Fig. 7a

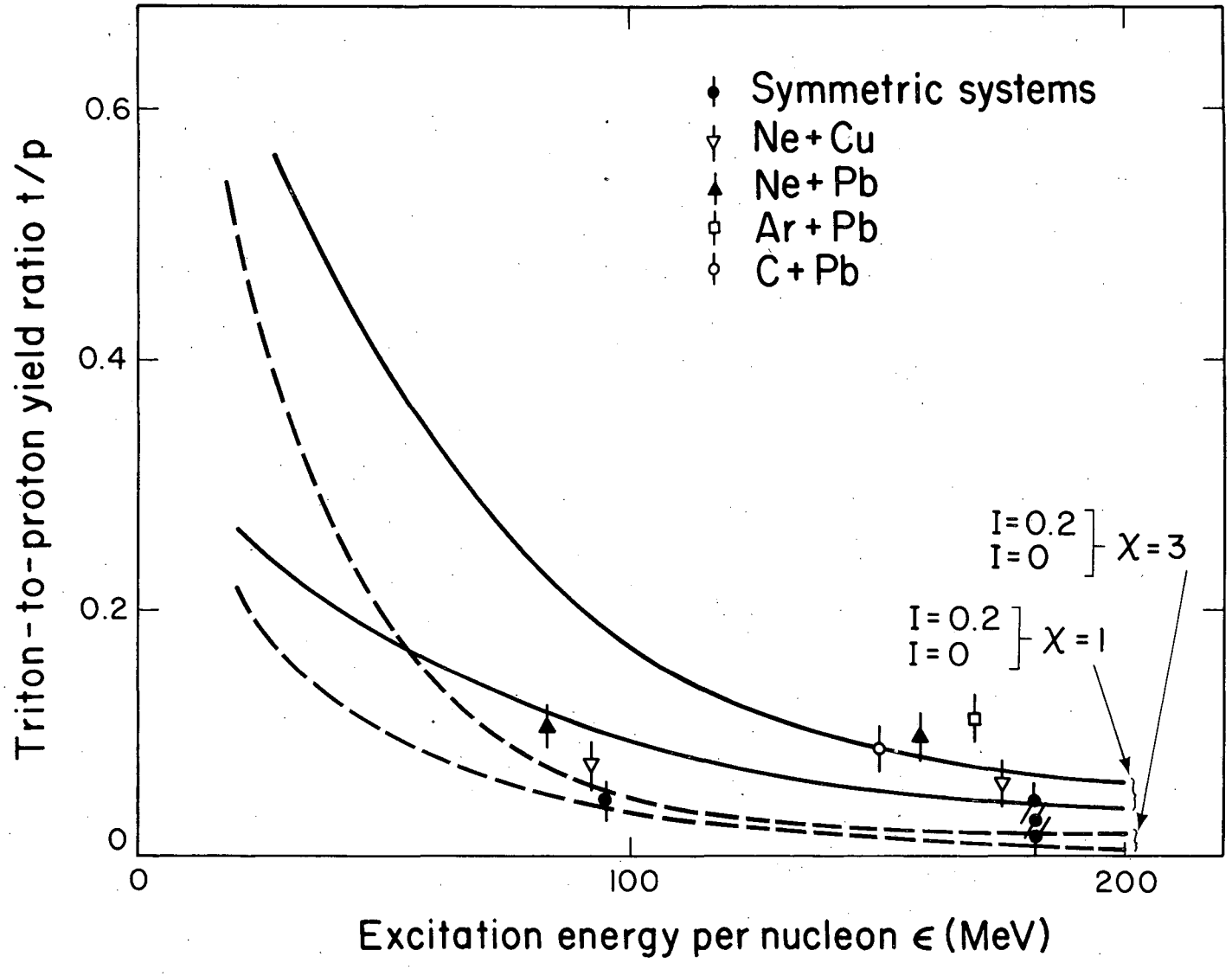

XBL 8110-1443

Fig. 7b

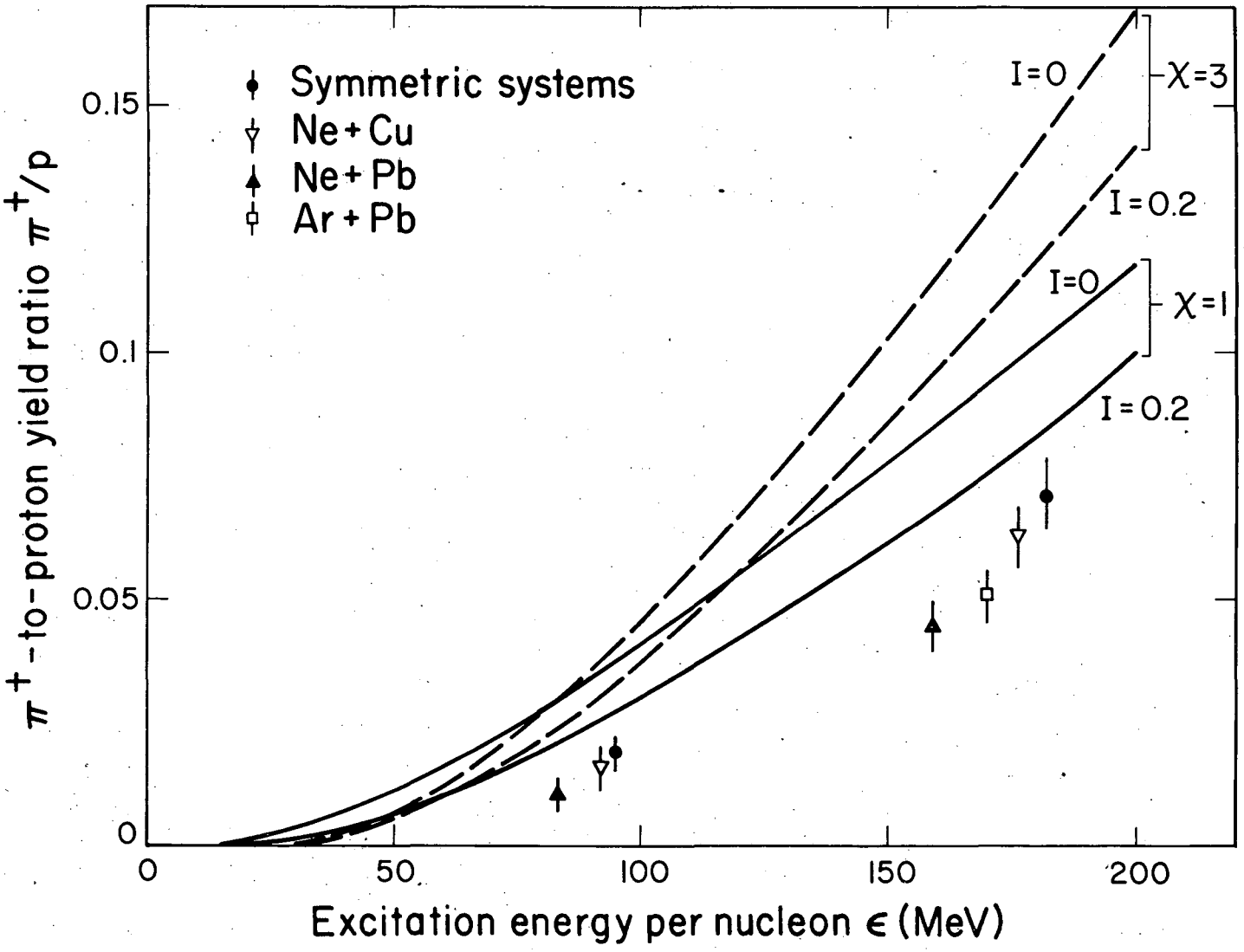

XBL 81.10-1444

Fig. 8a

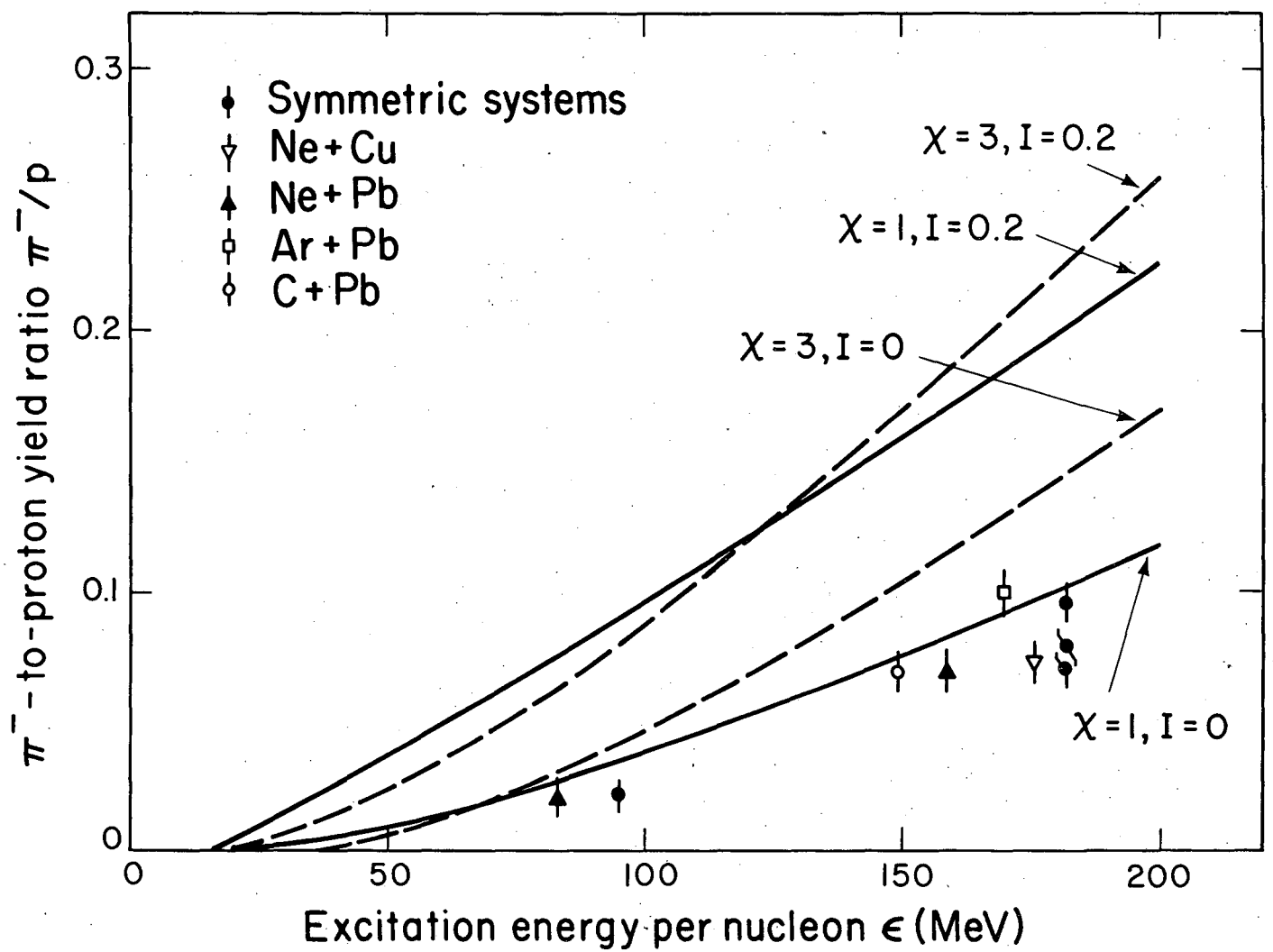

XBL 8110-1441

Fig. 8b

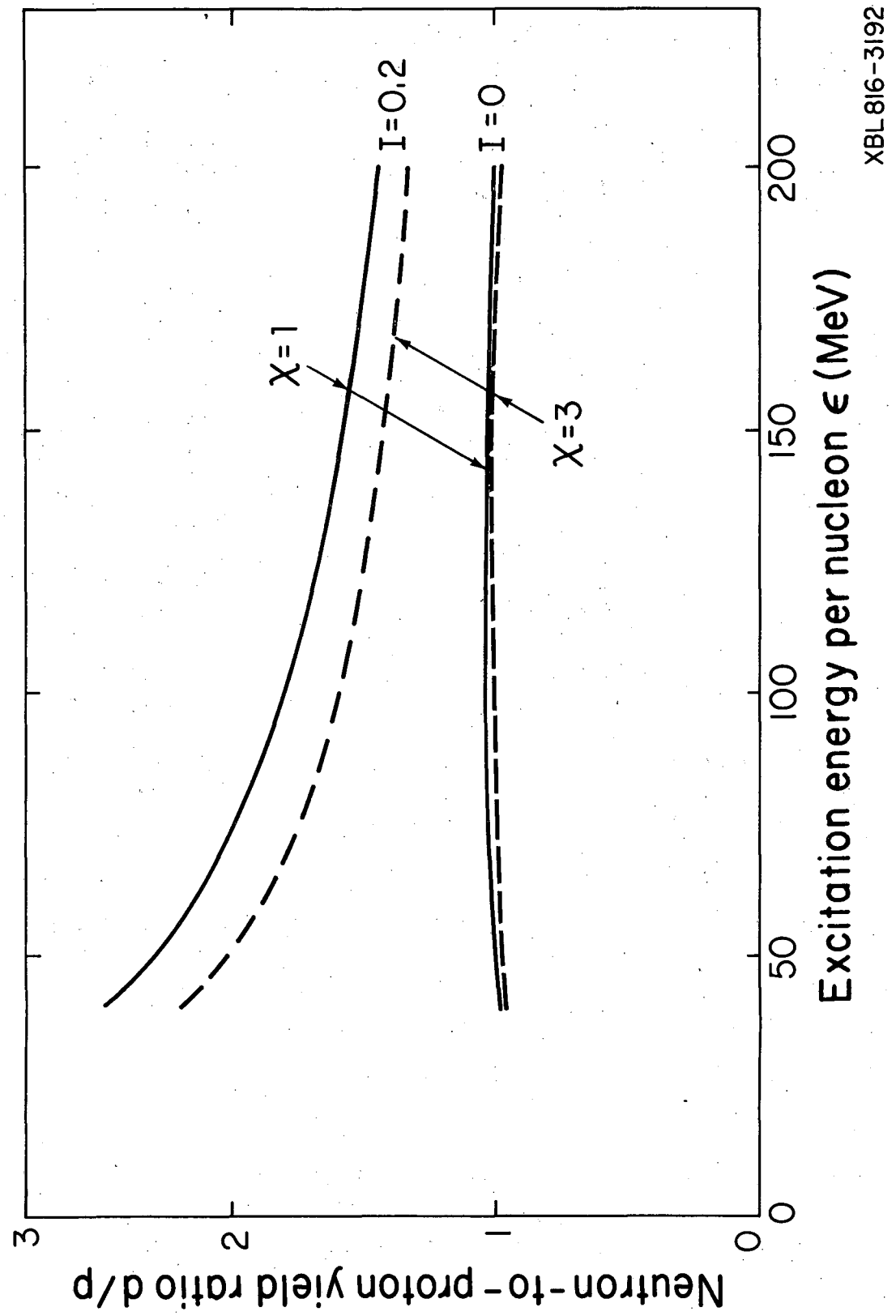

XBL816-3192

Fig. 9a

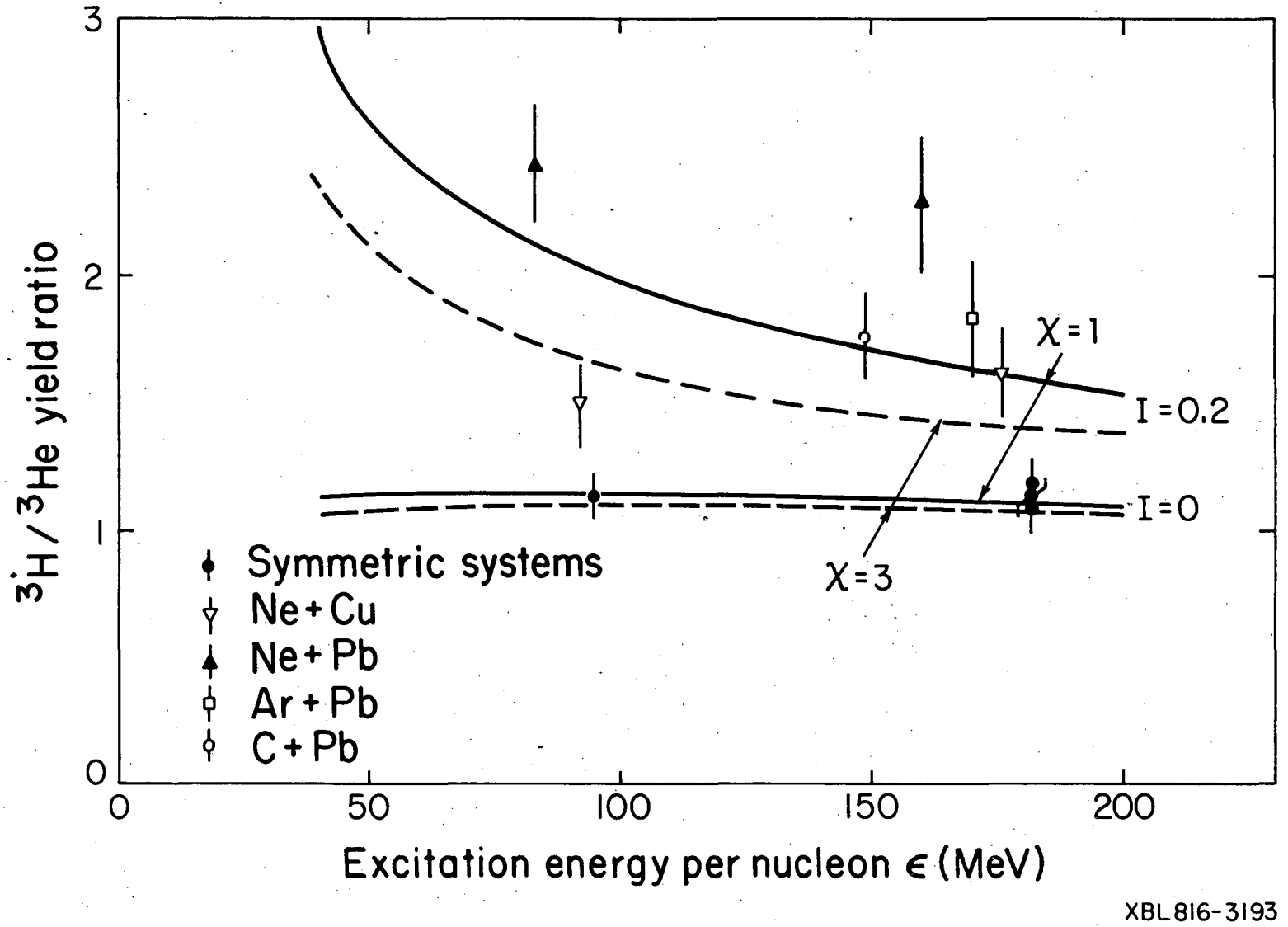
3
2
1
0
0
50
100
150
200
$^3H / ^3He$ yield ratio
Excitation energy per nucleon ϵ (MeV)
Symmetric systems
Ne + Cu
Ne + Pb
Ar + Pb
C + Pb
χ = 1
χ = 3
I = 0.2
I = 0
XBL816-3193

Fig. 9b

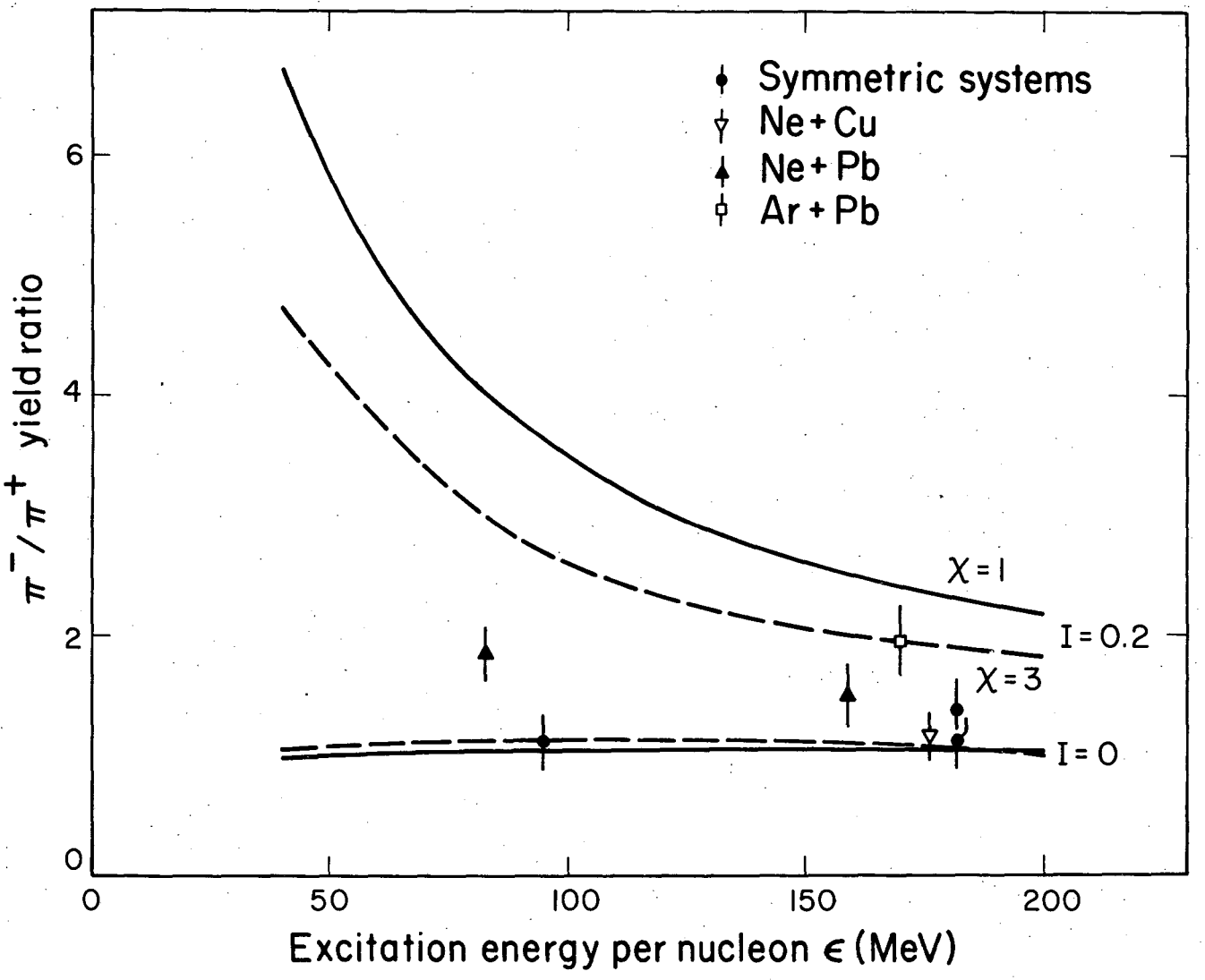
Symmetric systems
Ne+Cu
Ne+Pb
Ar+Pb
χ=1
I=0.2
χ=3
I=0
π^-/π^+ yield ratio
0
2
4
6
0
50
100
150
200
Excitation energy per nucleon ϵ (MeV)
XBL 8110-1440

Fig. 9c

This report was done with support from the Department of Energy. Any conclusions or opinions expressed in this report represent solely those of the author(s) and not necessarily those of The Regents of the University of California, the Lawrence Berkeley Laboratory or the Department of Energy.

Reference to a company or product name does not imply approval or recommendation of the product by the University of California or the U.S. Department of Energy to the exclusion of others that may be suitable.

TECHNICAL INFORMATION DEPARTMENT
LAWRENCE BERKELEY LABORATORY
UNIVERSITY OF CALIFORNIA
BERKELEY, CALIFORNIA 94720